Morphological change induced with NaOH–water solution for ramie fiber: change mechanism and effects of concentration and temperature

Nakano, Takato; Tanimoto, Takashi; Hashimoto, Tsuginosuke

Title: Morphological change induced with NaOH-water solution for ramie fiber: change mechanism and effects of concentration and temperature

Authors: Takato Nakano[1*], Takashi Tanimoto[2], Tsuginosuke Hashimoto[1]

Affiliation:

1: Laboratory of Biomaterials Design, Division of Forest and Biomaterials Science, Graduate School of Agriculture, Kyoto University

2: Asahi woodtech company

Chuoh-ku, Osaka, 541-0054, Japan

Address:

1: Kita-Shirakawa, Kyoto, 606-8502 Japan

2: Chuoh-ku, Osaka, 541-0054, Japan

***: Corresponding author**

e-mail: tnakano@kais.kyoto-u.ac.jp

Phone and Fax: +81-75-753-6234

Abstract:

The morphology of ramie fiber treated with NaOH-water solutions at various concentrations was observed with an epi-illumination microscope (EIM) equipped with a charge-coupled device (CCD) camera. The crystallinity was measured by X-ray diffraction. The morphological changes in length and width were quantified using image analysis. Changes in morphology were noted for samples treated with NaOH-water solutions at room temperature in the narrow concentration range of $0.08 < [NaOH] \leqq 0.12$. For samples cooled at –5°C after treatment, the morphological changes started at a lower concentration, i.e., at [NaOH] = 0.05. The change was observed as contraction in length and swelling in width. The mechanism for this dimensional change related closely not to the conformation of the whole microfibril but to the crystallinity of cellulose chains that had been de-crystallized by the NaOH-water solution: the calculated bond angle was too small for a zigzag conformation of the whole microfibril.

Keywords: Morphology, NaOH-water solution, Crystallinity, Cellulose microfibril, Contraction, Conformation

Introduction

Cellulose is the main constituent of wood and other plants, serving to maintain their structures and provide various physical properties. It is the greatest sustainable bioresource on earth. Native cellulose has a high crystallinity and is mostly found in plant cell walls as aggregates of cellulose microfibrils. These microfibrils have recently been categorized as nanofibers or nanocrystals [1]. In the present study, we quantified the morphological changes that occurred during treatment of ramie microfibrils with NaOH-water solution.

Native cellulose contains two crystalline forms, i.e., Iα and Iß. These forms can be transformed into other crystalline forms, such as cellulose II, via treatment with NaOH-water solution. Such polymorphic transformations have been discussed by many researchers [2-9]. O'Sullivan [10] attempted to bring and examine previous studies on cellulose structure over past few decades. The dissolution mechanism of cellulose during NaOH treatment has been studied by nuclear magnetic resonance (NMR) spectroscopy [11, 12]. Recently, Cai et al. [13-15] applied the method of Roy et al. [16] to the NaOH/urea and LiOH/urea systems. The latter authors used calorimetry, small X-ray scattering, and viscometry to study the structure of NaOH-water and cellulose-NaOH-water solutions in the range of various concentration, and proposed a mechanism that was appropriate at lower temperatures.

The morphological changes of cellulose that occur with NaOH-water treatment have been known for a long time. Davidson [17] and Sobue et al. [18] reported the effects of both concentration and temperature on qualitative changes in morphology. Watanabe et al. [19] also observed

crystallinity changes at low temperatures. Moigne et al. [20, 21] studied the morphological and swelling properties of native and regenerated cellulose from the viewpoint of cellulose solubility using water-soluble solvents such as NMMO (N-methylmorpholine-N-oxide). Although the crystalline transformations and dissolution of cellulose in alkali have been extensively studied, the quantitative evaluation of the morphological changes of the fibers during de-crystallization treatment has rarely been discussed, and its mechanism is poorly understood.

Stöchmann [22, 23] first reported the changes in morphology of wood pulp that occurred when it was treated with NaOH-water solutions and proposed a mechanism. Nakano [24, 25], Ishikura and Nakano [26], and Tanimoto and Nakano [27, 28] reported changes in the dimensional and mechanical properties of wood that occurred after treatment with NaOH-water solution; they attributed these changes to morphological changes in the microfibrils in the wood cell walls. Their results were later confirmed by Voronova et al. [29] and Ray and Sarkar [30]. Although many studies concerning treatments of wood and cellulose with NaOH-water solution have been reported, a quantitative description of the morphological changes of the microfibrils and fibers after treatment, particularly with respect to conformational changes, has not been reported to our knowledge.

The next subject of this work was to obtain quantitative, fundamental information on the conformation of microfibrils treated with NaOH-water solution. A goal was to model these conformational changes that occur during such treatment; the modeling and simulation results will be reported in a separate publication. Nishiyama et al. [31] and Sao et al. [32] examined the morphology of alkali-treated ramie in detail, but they focused on the changes in crystal structure and did not

establish a relationship between the macroscopic morphology and the conformation of the amorphous cellulose chains which is the structural arrangement. Thus, in the present work, conformational changes in the cellulose chains and in the whole microfibrils are discussed for ramie fiber partially de-crystallized by treatment with NaOH-water solution. These conformational changes were inferred from changes in their macroscopic morphologies and crystallinities.

Experimental

Materials and sample preparation

Purified ramie (commercial grade) was donated by Nichimen Kyokai. Samples of 10 ramie fibers cut about 2 mm long were treated with NaOH-water solution of different concentrations. The change in morphology of a sample was observed using an epi-illumination microscope (EIM) (Nikon Optiphoto, Tokyo, Japan) equipped with a charge-coupled device (CCD) camera. The magnification of the image was determined by a scale in the image; the magnification of the objective lens was always 5 ×.

To confirm the morphological changes in detail, the ramie fibers were continuously treated with NaOH-water solution at concentration fractions increasing from 0.00 to 0.20 (Experiment I). The same procedure was repeated several times to confirm reproducibility. In Experiment I, a sample was placed in distilled water and allowed to stand overnight at room temperature. The sample was then placed on a glass slide and excess liquid was removed. The sample was observed with the EIM and the CCD camera. After observation, the sample was placed in NaOH ([NaOH] = 0.03) and then allowed to equilibrate overnight at room temperature. This sample was observed by the EIM with the CCD

camera for a second time. The process was repeated with increasing NaOH concentration for [NaOH] ranging from 0.00 to 0.20. In this experiment, the immersion time increased with exposure to higher concentrations because the same sample had been exposed consecutively in solutions of increasing concentration.

Two other experiments (Experiments II and III) were conducted to observe the dependence of the morphology of the ramie fiber on NaOH concentration. In Experiment II, the sample was placed in NaOH-water solution at various concentration fractions ranging from 0.00 to 0.20 and was then allowed to stand for 1 week at room temperature. This sample was observed by EIM. After observation, the sample was rinsed for 1 week with distilled water and then observed again. In Experiment III, after the above NaOH treatment, the sample was held at –5°C for 1 day and then rinsed with distilled water for 1 week. Observation by EIM in Experiment III was done before and after the –5°C cooling treatment and after rinsing.

Overall, 15 conditions with 8 to 10 samples per [NaOH] condition were studied.

Measurement of morphological changes

Digital EIM images were transferred to a computer where Photostitch (Canon Co., Ltd.) and ImageJ (freeware) image analysis software were used to measure the lengths and widths of the ramie fibers. The length of a ramie fiber was calculated as the sum of the distances between points along its length. The width was calculated as the average of five locations where the fiber was not twisted.

Crystallinity

Samples that were cut to shorter lengths were treated with NaOH-water solutions at various concentrations by the above procedures, then rinsed with distilled water for 1 week, and oven-dried at 50°C under vacuum for 1 day. Pellets of approximately constant density were made from these samples using a molding machine. Diffraction patterns were obtained for these pellets at room temperature using an X-ray diffractometer (Rigaku Ultima IV) operating at 40 kV and 40 mA over a scanning range of 5–35° and at a scanning speed of 2°/min.

The crystallinity based on the X-ray diffraction measurement is generally calculated as the ratio of the intensity of crystalline cellulose to the total intensity or their area ratio. However, it is difficult to define the extent of conversion in crystalline region for both cellulose I and II using the same procedure because there is remarkable change in the profile and the effect of crystallite size on crystallinity index. Thus, some methods have been proposed [**33**]. Revol et al. [**34**] reported the effect of mercerization on crystallite size and crystallinity index. French and Cintron [**35**] also pointed out the effect of crystallite size on the Segal crystallinity index. The effect appears to be remarkable in the lower crystallinity estimated by the Segal method.

We examined some X-ray methods containing the Segal method and compared them with ^{13}C CP/MAS NMR method [**36**] where the crystallinity is calculated by expressing the area of the peak at 89 ppm as a ratio of the total area assigned to cellulose-C4. The X-ray method highly correlated with the NMR method was adopted, which had good agreement in the whole [NaOH] region containing the transformation region from cellulose I to cellulose II [**37**]: the coefficient of

138 determination was 0.869. The method estimates the crystallinity as below. The total intensity I_t and
139 the amorphous intensity I_a were confirmed from the peak height of the diffraction (200) and the
140 height of an intersection point where the perpendicular line through the peak (200) crosses the
141 straight line passing the specified point and $2\theta = 30°$, respectively: the specified point is the minimum
142 2θ between (1-10) and (200) for cellulose I and between (110) and (1-10) for transformation from
143 cellulose I to II and cellulose II. Then, the crystallinity was calculated using equation $(I_t - I_a)/I_t$.
144
145
146 **Results and discussion**
147 Morphological changes for non-cooled samples
148 **Figure 1(a)** shows the changes in the morphology of the ramie fiber as a function of NaOH
149 concentration. Few changes were observed for [NaOH] ≦ 0.05. A slight twist and contraction was
150 observed near [NaOH] = 0.10, while the width remained unchanged. However, significant changes in
151 length, width, and twist occurred for [NaOH] > 0.10.
152 The changes in length and width averaged over 8–10 samples are indicated by open circles
153 in **Figure 2(a) and (b)**, respectively. Their dimensions were accurately determined using image
154 analysis. Changes in the ramie fiber morphology, i.e., decreasing length and increasing width,
155 occurred over a narrow range of NaOH concentrations, i.e., 0.08 ≦ [NaOH] ≦ 0.12. These changes
156 corresponded to changes in the crystallinity (open circles in **Figure 3**). This [NaOH] range is similar to
157 that reported by Kamide et al. [38] and Yamane et al. [39]. No changes were observed at [NaOH] <

158 0.05 and [NaOH] > 0.12.

159 Although the concentration dependence (**Figure 2(a)**) was similar to those reported for
160 dimensional changes in the longitudinal direction of wood samples [**25, 40, 41**], the onset of the
161 changes was different. Contraction of a ramie fiber started at [NaOH] = 0.08, while for wood, it began
162 at a higher concentration of [NaOH] = 0.10. Additionally, changes in the ramie fiber leveled off at
163 [NaOH] > 0.12; this was not observed with wood.

164 In this study, the contraction of a ramie fiber treated with NaOH-water solution reached
165 nearly 0.30 point (**Figure 2(a)**), much greater than the reported 0.07 for wood [**36, 40**]. This substantial
166 difference is attributed to large structural differences. Microfibrils of ramie fiber are almost free in the
167 sense that they are not strongly restricted by other components, while microfibrils of wood are
168 embedded in a matrix such as hemicellulose and lignin. Moreover, the latter forms a helical structure
169 in the cell wall. In this connection, contraction of fibrillated cells reached 0.20 point after treatment
170 with NaOH-water solutions [**42**]. Revol and Goring [**2**] and Murase et al. [**3**] noted that lignin, which is
171 layered between microfibrils, limits the flexibility of cellulose chains and thereby the transformation of
172 cellulose I to cellulose II. The results shown as open circles in **Figure 2(a) and Figure 3** suggested that
173 the remarkable changes in morphology with NaOH treatment were closely related to crystallinity.

174 The concentration dependence of the morphological changes in fiber length and width after
175 rinsing is shown as closed circles in **Figures 2(a) and (b)**. After rinsing, the length barely changed,
176 while the width decreased markedly. However, the swelling in width remained at 0.30 point with
177 [NaOH] ≧ 0.12 even after rinsing. Both the induced contraction and residual swelling at the same

178 [NaOH] are attributed to the effect of an amorphous region created by the NaOH treatment. The
179 mechanism is discussed below.
180
181 Effect of cooling on morphological changes
182 The effect of cooling on morphological changes was examined in Experiment III. The effect of cooling
183 on the cellulose structure in cellulose-NaOH-water solution has been described by others. Davidson
184 [17] and Sobue et al. [18] observed the morphological changes and temperature dependence. Roy et al.
185 [16] examined in detail the structure in solution using various methods, such as small-angle X-ray
186 diffraction, viscosity, and differential scanning calorimetry (DSC) at low temperatures (–60 to 0°).
187 They proposed a model in which the cellulose-NaOH-water solution was composed of soda hydrates
188 bound to cellulose, with a "core" of nine free soda hydrates and free water. The solubility and swelling
189 of alkali-treated cellulose (e.g., by NaOH or LiOH) and NaOH/urea-water solutions are temperature
190 dependent, especially at low temperatures. Qi et al. [43] reported that the solubility of cellulose in such
191 solutions is strongly temperature dependent and that cellulose with a molecular weight of 10.0×10^4
192 dissolved completely in a solution pre-cooled to –12.6°C. Cai et al. [13] studied the rapid dissolution of
193 cellulose in aqueous LiOH/urea pre-cooled to –12°C and proposed a mechanism involving cleavage of
194 the chain packing of cellulose by LiOH hydrates through the formation of new hydrogen bonds. These
195 findings indicated that conformational changes of cellulose occurred in alkali solutions, even at low
196 temperatures. However, the effect of cooling on the morphological changes and solubility has not been
197 examined in detail.

198 Experiment III examined the effect of a low-temperature treatment on the morphological
199 changes in ramie. **Figure 1(b)** shows the changes that occurred during such treatment; cooling caused
200 a remarkable contraction in length and swelling in width.

201 **Figure 4** shows the changes in morphology found from Experiment III. The morphological
202 changes (open circles in **Figures 4(a) and (b)**) are similar to those found with Experiment II. This is
203 because the treatment before cooling in Experiment III was the same as that in Experiment II. The
204 morphological changes evident after cooling (crosses in **Figures 4(a) and (b)**) were quite different from
205 those found before cooling (open circles in **Figures 4(a) and (b)**). The concentration at which the
206 morphology changed shifted to lower concentration, i.e., the changes in length and width appeared at
207 $0.06 \leqq [NaOH] \leqq 0.12$. These morphological changes corresponded to changes in crystallinity (closed
208 circles in **Figure 3**). This suggested that the reduction in crystallinity caused the changes in
209 morphology, even under the conditions of Experiment III.

210 The morphological changes after rinsing were observed only in width, as in Experiment II.
211 The residual swelling under the cooling condition was greater than that in the absence of cooling,
212 probably because the former swelled more than the latter at the same NaOH concentration.

213

214 Changes in crystallinity line profile

215 **Figure 5(a)** shows the X-ray intensity line profiles of the ramie fibers, which corresponded to
216 the crystallinity changes shown in **Figure 3**. The changes in crystallinity profiles appeared in the same
217 [NaOH] region where the morphological changes occurred; no changes appeared at $[NaOH] \leqq 0.05$

and [NaOH] ≧ 0.12. **Figure 5(a)** also demonstrates that structural changes occurred with the transformation from cellulose I to II. The cellulose I pattern was observed for [NaOH] ≦ 0.10, while a pattern consistent with a mixture of cellulose I and II was seen for [NaOH] = 0.11. A higher cellulose II content was noted at [NaOH] ≧ 0.12. The pattern intensity for crystalline cellulose II at [NaOH] ≧ 0.12 was weaker than that for cellulose I at [NaOH] ≦ 0.10. This indicated a lower crystallinity. Comparison of the morphological changes shown in **Figures 2(a) and (b)** with the line profiles in **Figure 5(a)** clarified that a structural change of cellulose I to II caused the macroscopic changes in morphology. However, the transformation from cellulose I to II hardly affected the change in ramie length because there is only a slight difference in the length of their unit cells along the *c*-axis.

The X-ray diffraction profiles after cooling are shown in **Figure 5(b).** Cellulose I was found at [NaOH] ≦ 0.05, cellulose I and II co-existed at [NaOH] = 0.07, and cellulose II was clearly found at [NaOH] ≧ 0.08. The intensity decreased significantly in the transition region from cellulose I to II. The results of both Experiments II and III indicated that changing morphology was strongly related to changing crystallinity rather than to the transformation.

Figure 6 shows the relationship between crystallinity before and after cooling. The plots should lie on a linear as a broken line in **Figure 6**, if the NaOH treatment contributes equally to de-crystallization in both cases. However, it shows clearly that the [NaOH] region that induced the change in crystallinity differed for the two cases, i.e., the trajectory deviated from a straight line in the region of [NaOH], 0.07 ≦ [NaOH]≦ 0.12.

Morphological changes and microfibril conformation

Figure 7 shows the relationship between the morphology and crystallinity for samples in Experiments II and III. There were strong linear correlations between the length and crystallinity, and between the width and crystallinity, regardless of cooling or non-cooling and rinsing or non-rinsing. This linearity was clearly evident even for the width after rinsing (closed circles in **Figure 7(b)**).

The results shown in **Figure 7** demonstrate that the morphological changes in ramie fiber were related to crystallinity. There is a possibility that de-crystallization via NaOH treatment caused two conformational changes, i.e., changes to both the cellulose chains and to the microfibrils. Our interest is in the mechanism of the morphological changes, i.e., the cause of the contraction. Nakano et al. [**40**] and Nakano [**41**] proposed a mechanism concerning conformational changes induced by NaOH treatments.

The morphological changes in ramie can be understood in terms of Nakano's mechanism. First, NaOH-water solution attacks the periodic defects along the microfibrils and diffuses into the cross-sections. Periodic defects in microfibrils have been confirmed by a leveling-off of the degree of polymerization (LODP). Nishiyama [**31**] reported that microfibrils have 4-5 disordered residues for every 300 residues. Diffusing NaOH-water solutions creates amorphous regions. Crystalline and amorphous regions might co-exist in series after some time, even though initially the amorphous region is distributed. A part of the stretched cellulose chains in the crystalline microfibrils transform to random conformations; hence, the dimensions contract along the microfibrils. Thermodynamically,

this is an entropy-increasing process. That is, the driving force for the contraction is the entropic elastic force.

The above explanation, however, is based on the contribution of the conformational change in the cellulose chains alone. Our question was whether or not the conformational changes in the microfibrils alone contributed to the morphological changes. The residual swelling after rinsing provided insight. As shown by the closed circles in **Figure 2(b)**, the width after rinsing did not return to the initial value and the residual swelling increased with increased swelling immediately after NaOH treatment, i.e., with decreased crystallinity. The changes in length and width were highly correlated with crystallinity, even after rinsing (**Figure 7**). The length was not influenced by rinsing, while the width was strongly affected by rinsing. It should be noted that a residual swelling after rinsing was estimated at most 0.3 point. The answer to our question can be obtained by examination whether or not this value in width after rinsing allows the conformational changes in microfibrils alone.

Consider the probable conformational change in the microfibrils alone after rinsing: crystal and amorphous regions act as bonds and joints, respectively. We take up a symmetric zigzag conformation with 1° bond angle as an example. The size of bond width and joint is not considered to simplify our discussion. This example has a rod-like feature due to a small bond angle. If the width of this conformation is larger than a residual swelling in width, the significant conformational change in the microfibrils alone should hardly occur with NaOH treatment.

According to Nishiyama [31], the residues between periodic defects along ramie microfibrils is 300, and about 250 residues remain in the crystal region even after 0.2 point of the maximum

decrease in crystallinity as shown in **Figure 3**. The length is approximately 125 nm when the residue length is 0.52 nm and the bond angle of the β 1-4 ether linkages is not considered. Then, the increase in width is $125 \sin 0.5° = 1.09$ nm after the symmetric zigzag conformation with bond angle 1°. On the other hand, the maximum residual swelling 0.3 is corresponding to 0.6 to 1.8 nm and the average 1.2 nm, setting the microfibril width before the treatment 2 to 6 nm which is the general value for higher plant. The calculated value is nearly equal to the maximum residual swelling value, that is, the change in width of the zigzag conformation is close to the maximum value observed in our experiment, even if the bond angle is very small 1°. Consequently, significant conformational changes in the microfibrils are not expected with the NaOH treatment.

This implies that the amorphous regions created along the microfibrils during the NaOH treatment do not act as joints. Probably, the joints should have much lower flexibilities comparing with the β 1-4 ether linkages of the cellulose chains which have free rotation around the bonds. Thus, the conformation of the microfibrils may remain rod-like. Consequently, the morphological change is mainly attributed to the change in conformation of the cellulose chains de-crystallized via NaOH treatment. The schematic change is shown in **Figure 8**.

Conclusion

The morphology of ramie fiber treated with NaOH at various concentrations was observed by EIM equipped with a CCD camera. The changing crystallinity was documented by X-ray

298 diffraction. We proposed the following mechanism for the observed changes in morphology. First, the
299 NaOH-water solution attacks attacked the periodic defects along the microfibrils and diffused into the
300 cross-sections. Second, diffusing NaOH-water solutions created amorphous regions. Crystalline and
301 amorphous regions might co-exist in series after sufficient time has passed. The straight cellulose
302 chains in the crystalline microfibrils partially transforms into random conformations, resulting in
303 contraction along the microfibrils. However, significant conformational changes in the microfibrils are
304 not expected because the joints, which are amorphous regions created by the NaOH treatment, are
305 inflexible. Consequently, the morphological change is mainly attributed to the change in conformation
306 of the cellulose chains de-crystallized via NaOH treatment.
307
308
309 **Acknowledgments**

310 The authors thank Prof. Junji Sugiyama, Research Institute for Sustainable Humanosphere,
311 Kyoto University for providing the ramie.
312
313

References

[1]. Eichhorn, S.J., Dufresne, A., Aranguren, M., Marcovich, N.E., Capadona, J.R., Rowan, S.J., Weder, C., Thielemans, W., Roman, M., Renneckar,S., Gindl, W., Veigel, S., Keckes, J., Yano, H., Abe, K., Nogi, M., Nakagaito, A.N., Mangalam, A., Simonsen, J., Benight, A.S., Bismarck, A., Berglund, L.A., Peijs, T. (2010) Review; current international research into cellulose nanofibers and nanocomposites. J Mater Sc 45: 1-33.

[2]. Revol, J.-F., Goring, D.A.I. (1981) On the mechanism of the mercerization of cellulose in wood. J Appl Polym Sci 16: 1275-1282.

[3]. Murase, H., Sugiyama, J., Saiki, H., Harada, H. (1988) The effect of lignin on mercerization of cellulose in wood. Mokuzai Gakkaishi 34: 965-972.

[4]. Okano, T. and Sarko, A. (1984) Mercerization of cellulose I. X-ray diffraction evidence for intermediate structures. J Appl Polym 29: 4175-4182.

[5]. Okano, T. and Sarko, A. (1985) Mercerization of cellulose II. Alkali-cellulose intermediates and a possible mercerization mechanism. J Appl Polym 30: 325-332.

[6]. Hayashi, J., Yamada, T., Shimizu, Y.-L. (1989) Memory phenomenon of the original crystal structure in allomorphs of Na-cellulose. In Cellulose and Wood: Chemistry and Technology, Proceedings of the Tenth Cellulose Conference (C. Schuerch, ed.). New York; John Wiley and Sons, pp. 77-102.

[7]. Nishimura, H., Okano, T., Sarko, A. (1991a) Mercerization of cellulose 5, Crystal and molecular structure of Na-cellulose I. Macromolecules 24: 759-770.

[8]. Nishimura, H., Okano, T., Sarko, A. (1991b) Mercerization of cellulose 6. Crystal and molecular structure of Na-cellulose IV. Macromolecules 24: 771-778.

[9].Fengel, D., Jakob, H., Strobel, C. (1995) Influence of the alkali concentration on the formation of cellulose II. Holzforschung 49: 505-511.

[10]. O'sullivan, A.C. (1997) Cellulose: the structure slowly unravels. Cellulose 4: 173-207.

339 [11]. Kamide, K., Okajima, K., Kowsaka, K. (1985a) CP/MASS ^{13}C NMR spectra of cellulose Solids: An
340 explanation by the intramolecular hydrogen bond concept. Polymer J 17: 701-706.
341 [12]. Kamide, K., Kowsaka, K., Okajima, K. (1985b) Determination of intramolecular hydrogen bonds
342 and selective coordination of sodium cation in alkalicellulose by CP/MASS ^{13}C. Polymer J 17:
343 707-711.
344 [13]. Cai, J., Zhang, L. (2006) Unique gelation behavior of cellulose in NaOH/urea aqueous solution.
345 Biomacromolecules 7: 183-189.
346 [14]. Cai, J., Zhang, L., Chang, C., Cheng, G., Chen, X., Chu, B. (2007a) Hydrogen-bond-induced
347 inclusion complex in aqueous cellulose/LiOH/Urea solution at low temperature. Chem Phys
348 Chem 8: 1572-1579.
349 [15]. Cai, J., Zhang, L., Zhou, J., Qi, H., Chen, H., Kondo, T., Chen, X., Chu, B. (2007b) Multifilament
350 fibers based on dissolution of cellulose in NaOH/urea aqueous solution: structure and properties.
351 Adv Materials 19: 821-825.
352 [16]. Roy, C., Budtova, T, Navard, P., Bedue, O. (2001) Structure of cellulose – soda solutions at low
353 temperature. Biomacromolecules 2: 687-693.
354 [17]. Davidson G.F. (1934) The dissolution of chemically modified cotton cellulose in alkaline solution.
355 Part I; In solution of NaOH, particularly at T°C below the normal. J Text Inst 25: 174-196.
356 [18]. Sobue, H., Kiessing, H., Hess, K. (1934) The cellulose-sodium hydroxide-water system as a
357 function of the temperature. Z Physik Chem B 43: 309-328.
358 [19]. Watanabe, S., Kimura, K., Akahori, T. (1968) A study of mercerization of native cellulose by X-ray
359 method. Bulletin of the Faculty of Eng. Hokkaido University 47: 121-130.
360 [20]. LeMoigne N. and Navard, P. (2010a) Dissolution mechanisms of wood cellulose fibers in
361 NaOH-water Cellulose 17: 31-45.
362 [21]. LeMoigne, N., Bikard, J., Navard, P. (2010b) Rotation and contraction of native and regenerated
363 cellulose fibers upon swelling and dissolution: the role of morphological and stress unbalances.
364 Cellulose 17: 507-519.

365 [22]. Stöchmann, V.E. (1971a) Effect of pulping on cellulose structure Part I. Tappi 54: 2033-2037.

366 [23]. Stöchmann, V.E. (1971b) Effect of pulping on cellulose structure Part II. Tappi 54: 2038-2045.

367 [24]. Nakano, T. (1989a) Plasticization of wood by alkali treatment; Relationship between
368 plasticization and the ultra-structure (in Japanese). Mokuzai Gakkaishi (Journal of the Japan
369 Wood Research Society) 35: 431-437.

370 [25]. Nakano, T. (1989b) Plasticization of wood by alkali treatment; Effects of kind of alkali and
371 concentration of alkaline aqueous solution on stress relaxation (in Japanese). Nihon Reoroji
372 Gakkaishi (Journal of the Society of Rheology, Japan) 16: 104-110.

373 [26]. Ishikura, Y and Nakano, T. (2007) Contraction of the microfibrils of wood treated with aqueous
374 NaOH. J Wood Sci 53: 175-177.

375 [27]. Tanimoto, Y., Nakano, T. (2012) Stress relaxation of wood partially non-crystallized using
376 aqueous NaOH solutions. Carbohydrate Polymers 87: 2145-2148.

377 [28]. Tanimoto, Y., Nakano, T. (2013) Side-chain motion of components in wood samples partially
378 de-crystallized using aqueous NaOH solution. Carbohydrate Polymers 87: 2145-2148.

379 [29]. Voronova et al. (2004) Changes in the structure of flax cellulose induced by solutions of lithium,
380 sodium, and potassium hydroxides. Fiber Chemistry 36: 15-19.

381 [30]. Ray, D. and Sarkar, B.K. (2001) Characterization of alkali-treated jute fibers for physical and
382 mechanical properties. J Appl Polym Sci 80: 1013-1020.

383 [31]. Nishiyama, H, Kim, U., Kim, D., Katsumata, K., May, R.P., Langan P. (2003) Periodic disorder
384 along ramie cellulose microfibrils. Biomacromolecules 4: 1013-1017

385 [32]. Sao, K.P., Samantary, B, Bhattacherjee, S. (1996) X-ray line profile analysis in alkali-treated
386 ramie fiber. J Appl Polym Sci 60: 919-922.

387 [33] Mansikkamäki, P., Lahtinen, M., Rissanen, K. (2007)The conversion from cellulose I to cellulose II
388 in NaOH mercerization performed in alcohol-water systems: An X-ray powder diffraction study.
389 Carbohyd Polym 68: 35-43.

390 [34] Revol, J.F., Dietrich, A., Goring, D.A.I. (1987) Effect of mercerization on the crystallite size and

crystallinity index in cellulose from different sources. Can J Chem 65: 1724-1727.

[35] French, A.D., Cintron, M.S. (2013) Cellulose polymorphy, crystallite size, and the Segal crystallinity Index. Cellulose 20: 583-588.

[36] Horii, F., Hirai, A., Kitamura, R. (1982) Solid-state high-resolution ^{13}C-NMR studies of regenerated cellulose samples with different crystallinities. Polym Bull 8: 163-170.

[37] Miura, K., Nakano, T. (2012) T. Abstracts of the 62rd Annual meeting of the Japan Wood Research Society. K16-06-1015.

[38]. Kamide, K., Okajima, K., Kowsaka, K. (1992) Dissolution of natural cellulose into aqueous alkali solution: role of super-molecular structure of cellulose. Polymer J 24: 71-86.

[39]. Yamane, C., Saito, M., Okajima, K. (1996) Industrial preparation method of cellulose-alkali dope with high solubility. Senni Gakkaishi (Journal of the Society of Fiber Science and Technology, Japan) 52: 310-317.

[40]. Nakano, T., Sugiyama J., Norimoto M. (2000) Contraction force and transformation of microfibril with aqueous sodium hydroxide solution. Holzforschung 54: 315-320.

[41]. Nakano, T. (2010) Mechanism of microfibril contraction and anisotropic dimensional changes for cells in wood treated with aqueous NaOH solution. Cellulose 17: 711-719.

[42]. Watanabe, T., Nakano, (2012) T. Abstracts of the 62nd Annual meeting of the Japan Wood Research Society. A 16-02-1500.

[43]. Qi, H., Chang, C., Zhang, L. (2008) Effects of temperature and molecular weight on dissolution of cellulose in NaOH/urea aqueous solution. Cellulose 15: 779-787.

413 **Captions:**

414 Figure 1. Typical morphological changes for ramie fiber treated with various NaOH-water
415 concentrations at room temperature (a) and with [NaOH] = 0.07 at –5°C (b).

416 Figure 2. Changes in length (L/L_0) and width (W/W_0) of ramie fiber treated with various NaOH-water
417 concentrations at room temperature (○, before rinsing; ●, after rinsing).

418 Figure 3. Changes in crystallinity of ramie fiber treated with various NaOH-water concentrations at
419 room temperature (○) and –5°C (●).

420 Figure 4. Changes in length (L/L_0), width (W/W_0) of ramie fiber treated with various NaOH-water
421 concentrations at room temperature followed by cooling and then rinsing (○, before cooling; ×,
422 after cooling; ●, after rinsing).

423 Figure 5. Dependence of X-ray profiles of treated samples on NaOH concentration for non-cooling and
424 cooling treatments.

425 Figure 6. Relationship between crystallinity before and after cooling for samples treated with
426 NaOH-water solution.

427 Figure 7. Crystallinity dependence of changes in length (L/L_0) and width (W/W_0) for samples treated
428 with NaOH-water solution (○, before rinsing; ●, after rinsing).

429 Figure 8. Schematic diagram showing the morphological changes in microfibrils treated with
430 NaOH-water treatment.

431

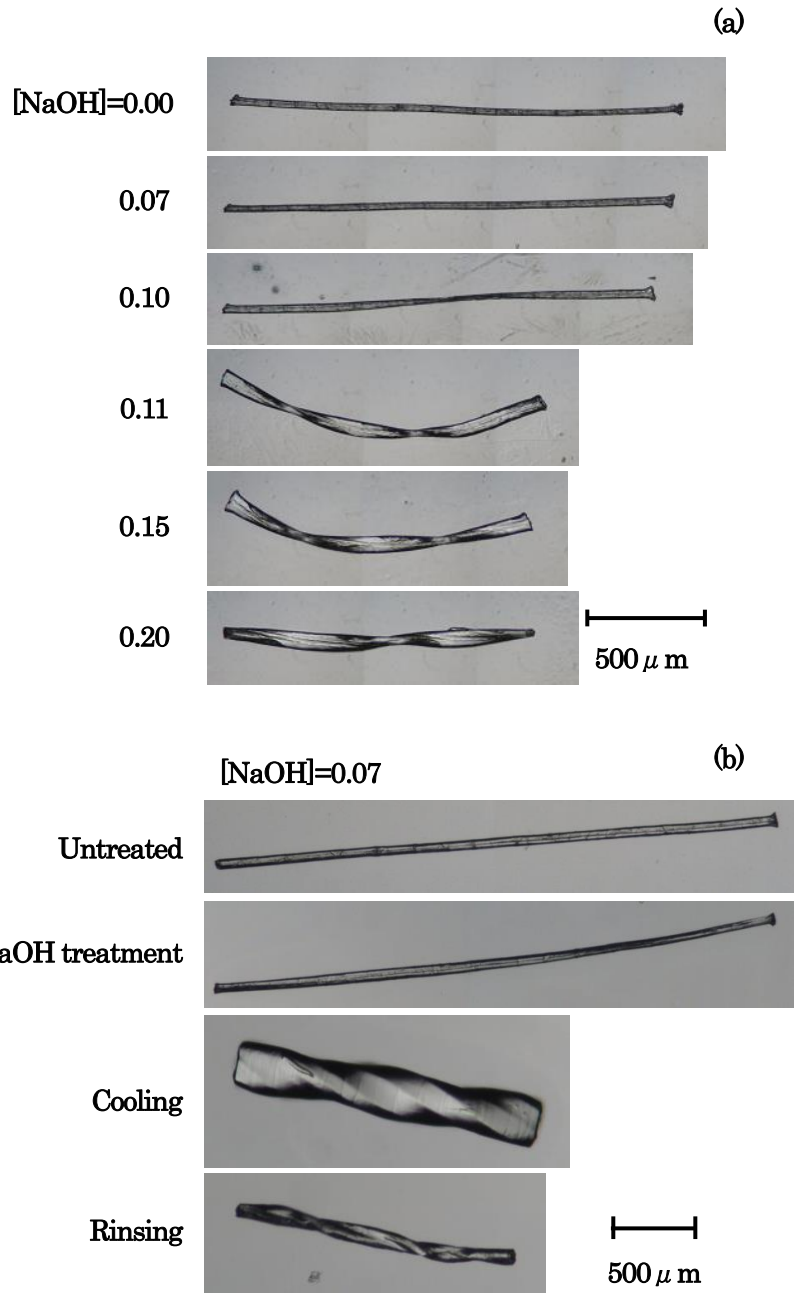

Figure 1.

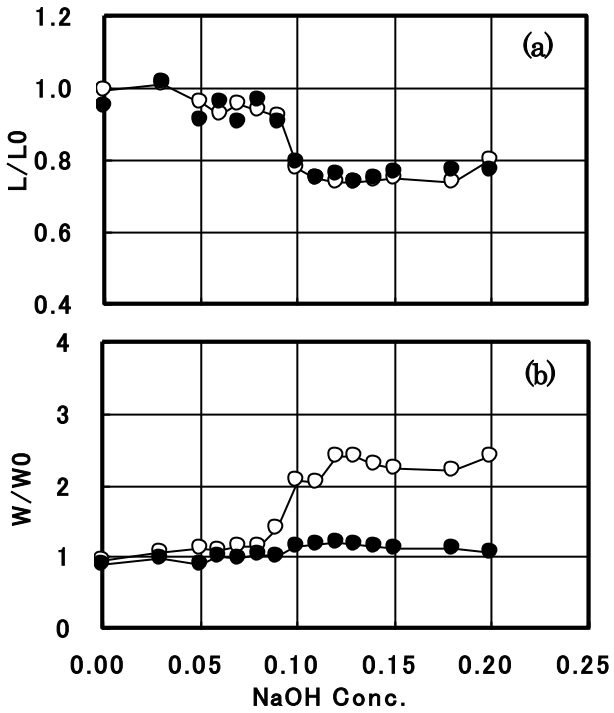

Figure 2.

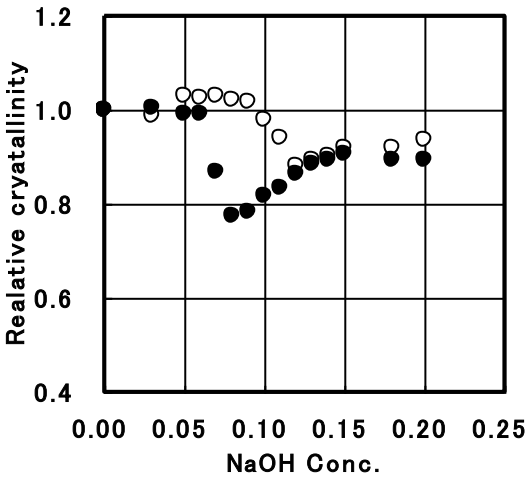

Figure 3

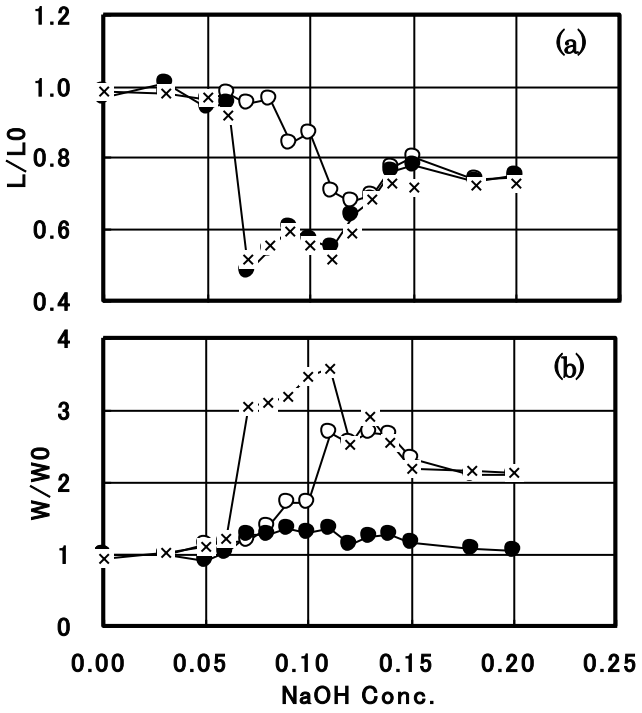

Figure 4.

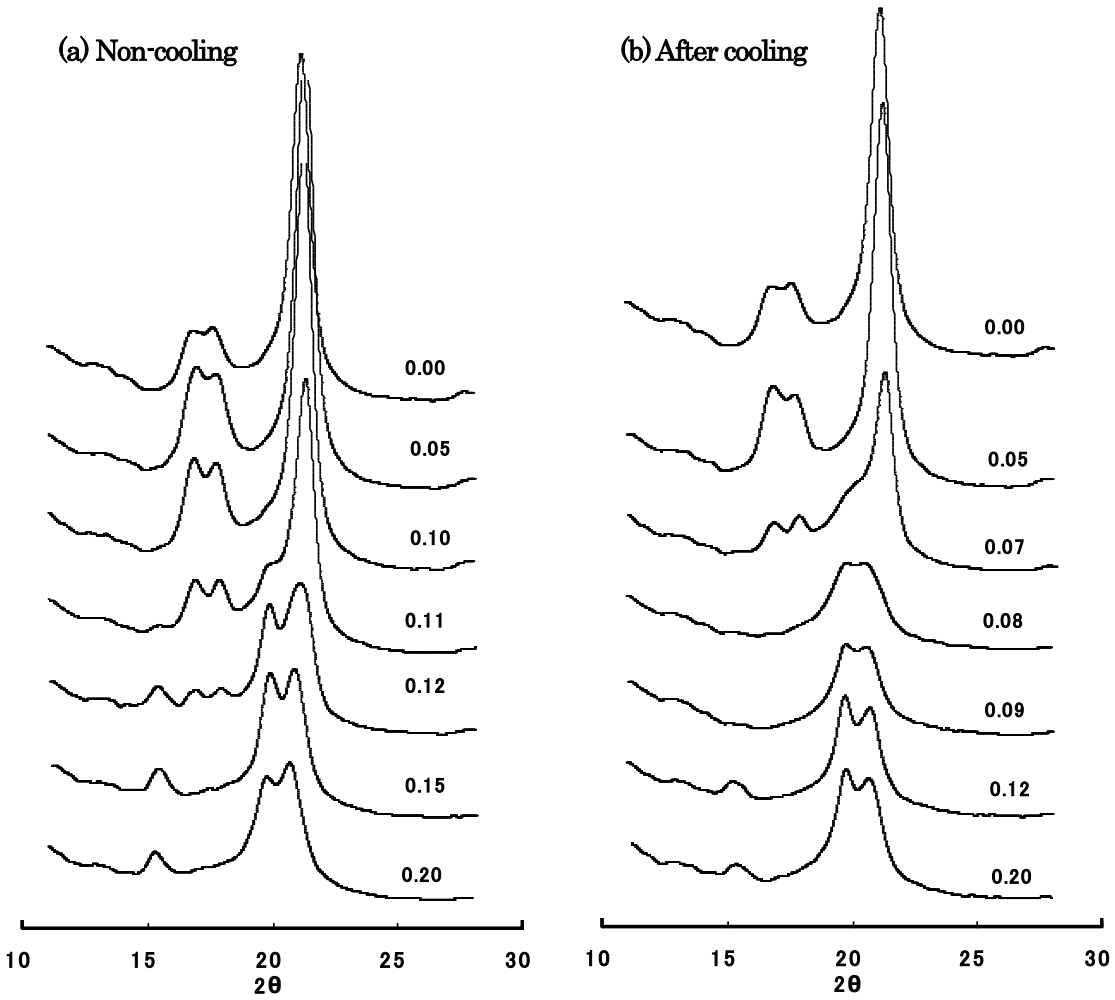

Figure 5.

514

515

516

517

518

519

520

521

522

523

524

525

526

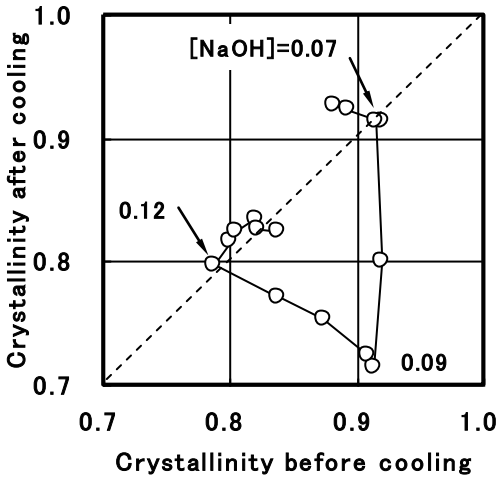

527 Figure 6.

528

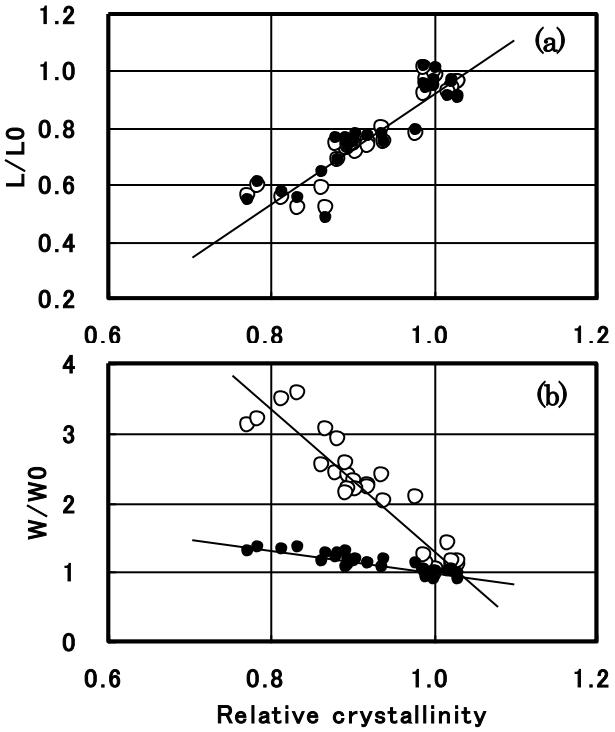

Figure 7.

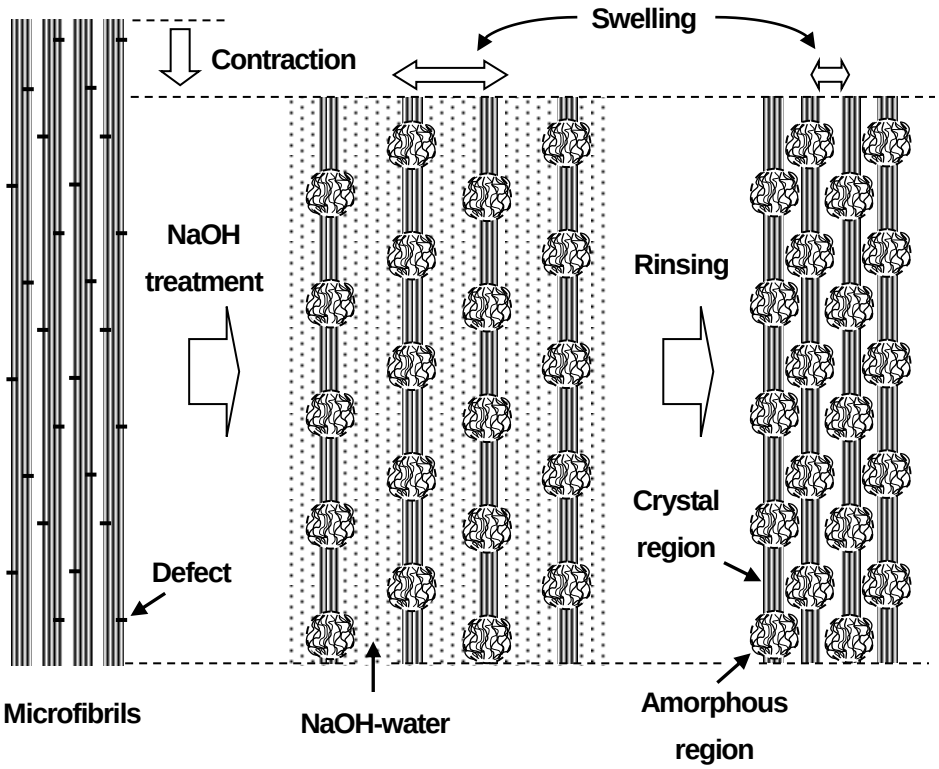

Figure 8.